In Joint Conference 8th IFAC Symposium on Mechatronic Systems and 11th IFAC Symposium on Nonlinear Control Systems, Vienna, Austria, 2019

Multi-Layer Spatial Iterative Learning Control for Micro-Additive Manufacturing ⋆

Leontine Aarnoudse * **Christopher Pannier** **
Zahra Afkhami ** **Tom Oomen** * **Kira Barton** **

* *Dept. of Mechanical Engineering, Eindhoven University of Technology, 5600 MB Eindhoven, The Netherlands (e-mail: l.i.m.aarnoudse@student.tue.nl).*
** *Dept. of Mechanical Engineering, University of Michigan, Ann Arbor, MI 48109, USA (e-mail: pannier@umich.edu)*

Abstract: Spatial iterative learning control (SILC) has been used in the control of additive manufacturing systems that can be described by their spatial dynamics. Since the current framework is limited to single-layer parts, the aim of this paper is to provide an approach to multi-layer SILC using learning in the layer-to-layer dimension. Mathematical formulation of a multi-layer SILC controller is provided, and active feedback control is demonstrated to reduce the error accumulation over the iterations. Simulation results using a model of high-resolution e-jet printing verify performance improvements for the proposed framework.

Keywords: Learning Control, Micro-Additive Manufacturing, Control Applications, Feedback Control, Spatial Domain

1. INTRODUCTION

Micro-additive manufacturing systems based on jet printing are used to fabricate functional electronics, sensors, and applications in the field of biotechnology, for example lab-on-a-chip devices (Onses et al. (2015)). Performance of these devices depends on the accurate construction of the device geometry. Traditional feedback control cannot be used for control of the printed geometry because real-time surface sensing is not feasible at this length scale, however the printed surface can be scanned after curing a layer. Commercial inkjet additive manufacturing systems lack topography feedback and use a subtractive milling process, although new concepts for closed-loop topography control are emerging in research (Sitthi-Amorn et al. (2015); Guo et al. (2017)). Because of the lack of real-time feedback, new strategies for purely additive control of the printed part geometry are needed to improve manufacturing yield and precision.

Spatial iterative learning control (SILC) is a model-based feedforward technique for deposited topography control. In SILC, two-dimensional convolution is used to describe the spatial spread of build material using the coupling of each discrete point in the x,y-plane to its neighbors (Hoelzle and Barton (2016)). Models of drop formation (Carter et al. (2014)) and spread (Pannier et al. (2017)) have been developed, but layer-to-layer dynamics are not well understood. Therefore plant models are based on system identification for a limited set of topographies (Wang et al. (2018b)). The SILC framework considers the part geometry to be a heightmap and has been successfully applied to electrohydrodynamic jet (e-jet) printing for single-layer prints (Wang et al. (2018a)).

Although multi-layer micro-scale additive manufacturing is increasingly important, at present SILC is formulated for single layers only. Single-layer parts are limited in the maximum height that can be achieved, whereas a multi-layer framework allows for more freedom in reference geometry design and hence more part applications. Many micro-additive manufacturing device applications consist of multiple layers, and material deposition preciseness can be improved by dividing a structure in multiple layers.

The aim of this paper is to extend SILC to a multi-layer framework. This extension is limited to parts consisting of layers with identical heightmaps and materials. Since the multi-layer parts that are considered consist of repeating layers, learning within the part is possible. Small variances in the printed layer are captured through an iteration- and spatially-varying impulse response that describes the system behavior as a function of the previous layer topography. Robustness for iteration-varying system behavior has been examined for broad applications (Altin et al. (2017); Meng and Moore (2017)). These conditions are reviewed for the system considered here. An important consideration in multi-layer SILC is the accumulation of the total topography error from layer-to-layer. A method for reducing this accumulation is through the use of a feedback pass. The multi-layer SILC framework is designed to enable activation of such a mechanism. The contribution of this paper is threefold:

(1) A framework for multi-layer SILC using learning within the part is presented and the iteration-varying system behavior is addressed.

⋆ This work is supported by the U.S. National Science Foundation under Grant Nos. GRFP-1256260 and CMMI-1434693.

(2) Feedback is implemented in separate passes, allowing correction of the accumulated error.
(3) The proposed framework with the feedback implementation is validated in simulations.

This paper is organized as follows. In Section 2 notation is introduced. In Section 3 the design problem is defined. The multi-layer SILC framework, as well as a way to implement feedback passes to correct the accumulated error, is presented in Section 4. In Section 5 the numerical simulations and their results are presented. Conclusions and future directions are presented in Section 6.

2. PRELIMINARIES

We take $\mathbb{Z}$ to represent the set of integers and $\mathbb{N}$ to represent the set of nonnegative integers. For any matrix $\mathbf{M}$, $\|\mathbf{M}\| = \sqrt{\sum_{i=1}^{m}\sum_{j=1}^{n}|a_{ij}|^2}$ denotes the Frobenius norm. The following definitions are used.

- A plant is said to be bounded input, bounded output (BIBO) stable if given an input function with finite magnitude $|f(x,y,t)| < \alpha$ for $t > 0$ and all x and y, the output has a finite magnitude $|g(x,y,t)| < \beta$ for $t > 0$ and all x and y, with $\alpha, \beta \in \mathbb{R}^+$.
- If $\lim_{k\to\infty}\|x_k - v_k\| = 0$ for any norm, x is said to converge to v.
- If $\lim_{k\to\infty}\sup\|x_k - v_k\| < \infty$ for any norm, x is said to converge to a bounded neighborhood of v
- An ILC update law with updates f_j is said to be monotonically convergent in the l_2-norm if $\|f_\infty - f_{j+1}\| \leq k\|f_\infty - f_j\| \quad \forall j \in \mathbb{N}$ for some $k \in [0,1)$.
- A matrix $\mathbf{H}$ lies in a neighborhood of a nominal matrix $\bar{\mathbf{H}}$ if there exists a finite real constant ρ so that $\|\mathbf{H} - \bar{\mathbf{H}}\| < \rho$.

3. PROBLEM DEFINITION

The aim of this paper is to develop an SILC approach to additively manufacture multi-layer parts consisting of identical layers of a single material. First, the plant model for the micro-additive manufacturing system is presented. Secondly, the suitability of SILC for this type of system is explained.

3.1 Plant model

Consider an additive manufacturing system as described in Hoelzle and Barton (2016). The plant is causal in time and non-causal in space, meaning that an applied input at a spatial coordinate will influence the output at advanced coordinates. The spatiotemporal dynamics of the plant can be simplified to be purely spatial, and the system is bounded input, bounded output (BIBO) stable. The additive manufacturing system is modelled using a heightmap evolution model (Pannier et al. (2019)), resulting in the spatially non-causal convolution equation

$$g_{k+1}(x,y) = g_k(x,y) + \sum_{\substack{m\in\mathbb{Z}\\ n\in\mathbb{Z}}} h_{k+1}^{(m,n)}(x-m, y-n) f_{k+1}(m,n) \tag{1}$$

where input f_k is an array of drop sizes, output g_k is a heightmap and $h_k^{(m,n)}$ is the impulse response at location

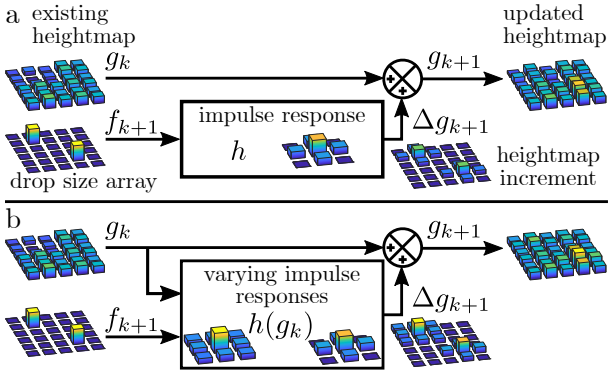

Fig. 1. Heightmap evolution model for a constant impulse response (a) and a topography-dependent impulse response (b).

(m,n) for each layer k. All 2D signals have finite support. The impulse response depends strongly on the surface on which the material is printed. Since layers are printed on top of each other, h_{k+1} is a function of the previous layer topography g_k as shown in Fig. 1. The system can be written in lifted form

$$\mathbf{g}_{k+1} = \mathbf{g}_k + \mathbf{H}(\mathbf{g_k})\mathbf{f}_{k+1} \tag{2}$$

where $\mathbf{f}_k$ and $\mathbf{g}_k$ are the row-wise vectorizations of f_k and g_k. In the multi-layer SILC approach we will consider a part consisting of multiple layers. The system is described in terms of the height change of these layers $\Delta\mathbf{g}_k$ instead of the total height map $\mathbf{g}_k$:

$$\Delta\mathbf{g}_{k+1} = \mathbf{g}_{k+1} - \mathbf{g}_k = \mathbf{H}(\mathbf{g}_k)\mathbf{f}_{k+1} \tag{3}$$

3.2 Spatial Iterative Learning Control

Iterative learning control is a control method whereby the feedforward input signal is modified based on preceding experiments that use the same reference, so that the norm of the tracking error is reduced. In traditional ILC, the assumption of constant plant and reference over iterations is crucial.

The main difference between SILC and temporal ILC is that SILC is based on spatial coordinates. This makes it suitable for additive manufacturing systems that use raster trajectories. In these trajectories two points can be close in space, yet distant in time. In SILC, two-dimensional convolution is used to describe the spatial dynamics as the spread of material using the coupling of each coordinate to its neighbors. The spatial distribution of material is a function of the heightmap of the neighboring locations. SILC can be described in a form similar to the lifted ILC framework for temporal systems.

4. MULTI-LAYER SPATIAL ITERATIVE LEARNING CONTROL

For a multi-layer part consisting of repeating layers, SILC learning over these layers is possible. In this vertical learning approach to multi-layer SILC, each layer is an iteration of the SILC system, as shown in Fig. 2. The topography error accumulates over layers, causing iteration-varying system behavior as well as an accumulated deviation from the desired final height h_{des}. This section provides the

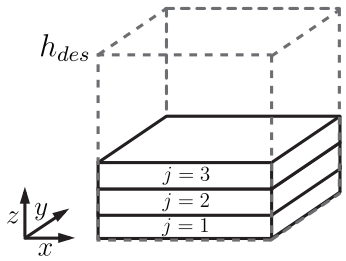

Fig. 2. Multi-layer part consisting of repeating topography across layers.

multi-layer SILC framework for vertical learning, the conditions for stability and convergence and the controller design. To address the accumulation of the topography error, the implementation of feedback printing passes is proposed and the controller choice for this feedback is discussed.

4.1 Framework

The desired topography $\Delta\mathbf{g}_d$ is identical for all n layers. Since the part has a target total topography $h_{des} = n\Delta\mathbf{g}_d$, the number of iterations within one part is limited. This is different from conventional ILC, where there is no limit to the number of iterations. To apply vertical SILC, it is assumed that a single material is used for each layer, and that the total thickness of previous layers does not influence the spatial impulse response of the system. Since each layer k is one iteration of the SILC loop, the system dynamics can be rewritten as follows in terms of the iterations j:

$$\Delta\mathbf{g}_{j+1} = \mathbf{H}(\mathbf{g}_j)\mathbf{f}_{j+1} \tag{4}$$

The feedforward input signal $\mathbf{f}_{j+1}$ is calculated from the filtered input signal $\mathbf{f}_j$ and error $\mathbf{e}_j$ from the previous iteration. The multi-layer SILC update law (Fig. 3) is given by:

$$\mathbf{f}_{j+1} = \mathbf{L}_f\mathbf{f}_j + \mathbf{L}_e\mathbf{e}_j = (\mathbf{L}_f - \mathbf{L}_e\mathbf{H}(\mathbf{g}_{j-1}))\mathbf{f}_j + \mathbf{L}_e\Delta\mathbf{g}_d \tag{5}$$

With filters $\mathbf{L}_f$ and $\mathbf{L}_e$. The error is defined as

$$\mathbf{e}_j = \Delta\mathbf{g}_d - \Delta\mathbf{g}_j \tag{6}$$

where $\Delta\mathbf{g}_d$ is the desired output for a single layer and $\Delta\mathbf{g}_j$ is the actual output for that layer.

In addition to the iteration-varying plant matrix, a nominal system is defined. The nominal system behavior $\bar{\mathbf{H}}$ is the plant matrix that results from the desired topography: $\bar{\mathbf{H}} = \mathbf{H}(\mathbf{g}_d)$. For the nominal system, it holds that $\mathbf{H}_j = \bar{\mathbf{H}} \quad \forall j \in \mathbb{N}$.

Because of the finite target height of the part, the number of iterations within one part is limited. However, the multi-layer SILC can be extended to a multi-layer, multi-part SILC framework. A second part can take advantage of the learning from the previous part, by starting at an iteration $j > 1$ using the last SILC update from the previous part.

4.2 Stability & convergence

The iteration-varying system behavior influences the stability and convergence conditions of the update law (5). Under certain conditions regarding the boundedness of the variations, Altin et al. (2017) have shown stability and convergence of the update law.

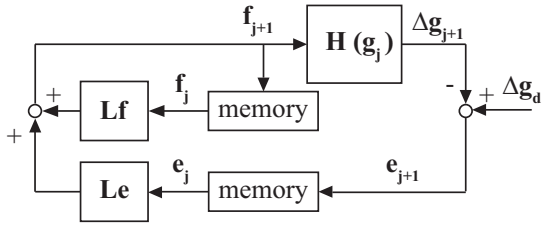

Fig. 3. Block diagram of SILC.

It is assumed that the plant matrices $\mathbf{H}_{j+1} = \mathbf{H}(\mathbf{g}_j)$ lie in a neighborhood of the nominal plant $\bar{\mathbf{H}}$ for all $j \in \mathbb{N}$. The filters $\mathbf{L}_f$ and $\mathbf{L}_e$ are selected to meet the robustness condition

$$\|\mathbf{L}_f - \mathbf{L}_e\mathbf{H}_j\| \leq \gamma < 1, \quad \forall j \in \mathbb{N}. \tag{7}$$

In the case of nominal system behavior, the robustness condition (7) guarantees monotonic convergence. If these assumptions hold, the SILC update law (5) is asymptotically and BIBO stable. The input and error of the iteration-varying system converge to a bounded neighborhood of the nominal input and error $\bar{\mathbf{f}}$ and $\bar{\mathbf{e}}$, and the system output $\Delta\mathbf{g}_j$ is bounded. If $\mathbf{H}$ converges to $\bar{\mathbf{H}}$, then $\mathbf{f}$ and $\mathbf{e}$ converge to $\bar{\mathbf{f}}$ and $\bar{\mathbf{e}}$.

In the multi-layer additive manufacturing application considered in this work, layers are printed directly on top of each other. As such, heightmap errors accumulate from one layer to the next, unlike SILC across multiple parts (Hoelzle and Barton (2016)). The framework and stability analysis provided in this work hold for a spatially- and iteration-varying model, with the assumption that the model variations are small so that the system converges to a small neighborhood of the nominal system behavior.

4.3 Norm-optimal SILC

The update law used for the system described in the previous two sections should be robust against plant uncertainties (Altin et al. (2017)). One approach to selecting the filters is norm-optimal SILC. In norm-optimal SILC, the following cost function is minimized:

$$\mathcal{J} = \mathbf{e}_{j+1}^T\mathbf{Q}\mathbf{e}_{j+1} + \mathbf{f}_{j+1}^T\mathbf{S}\mathbf{f}_{j+1} + (\mathbf{f}_{j+1} - \mathbf{f}_j)^T\mathbf{R}(\mathbf{f}_{j+1} - \mathbf{f}_j) \tag{8}$$

where the weight matrices $\mathbf{Q}$, $\mathbf{S}$ and $\mathbf{R}$ are user-defined positive definite matrices to obtain performance and robustness objectives such as attenuation of trial-varying disturbances ($\mathbf{R}$). These matrices are commonly chosen to be scaled identity matrices: $\mathbf{Q} = q\mathbf{I}$, $\mathbf{S} = s\mathbf{I}$ and $\mathbf{R} = r\mathbf{I}$. The norm-optimal filters $\mathbf{L}_f$ and $\mathbf{L}_e$ that minimize this cost function for the nominal plant $\bar{\mathbf{H}}$ are given by:

$$\mathbf{L}_f = (\bar{\mathbf{H}}^T\mathbf{Q}\bar{\mathbf{H}} + \mathbf{S} + \mathbf{R})^{-1}(\bar{\mathbf{H}}^T\mathbf{Q}\bar{\mathbf{H}} + \mathbf{R}) \tag{9}$$

$$\mathbf{L}_e = (\bar{\mathbf{H}}^T\mathbf{Q}\bar{\mathbf{H}} + \mathbf{S} + \mathbf{R})^{-1}\bar{\mathbf{H}}^T\mathbf{Q} \tag{10}$$

The derivation of these learning filters follows along the lines of the derivation in Gunnarsson and Norrlöf (2001). The final error in the case of nominal system behavior without disturbances is given by:

$$\mathbf{e}_\infty = (\mathbf{I} - \bar{\mathbf{H}}(\bar{\mathbf{H}}^T\mathbf{Q}\bar{\mathbf{H}} + \mathbf{S})^{-1}\bar{\mathbf{H}}^T\mathbf{Q})\mathbf{g}_d \tag{11}$$

The final error and the convergence behavior depend on the weighting matrices. To obtain the desired SILC

behavior, the weighting matrices for $\mathbf{L}_f$ and $\mathbf{L}_e$ can be tuned.

4.4 Feedback implementation

As discussed, additive manufacturing involves layers printed directly on top of each other, allowing printing errors not compensated by SILC to accumulate from layer-to-layer. Despite the lack of in-layer monitoring, the total layer height can be measured at the end of each printed layer cycle. Once the total topography error reaches a critical amount, a *feedback* iteration can be implemented. To compensate for actuator saturation limits and improve the sensitivity of the feedback correction, the feedback error compensation is combined with the most recent SILC input. Importantly, this combined layer does not contribute to the *learning* process, hence $g_j = g_{k+1}$. Since the feedback pass is implemented outside of the SILC loop, it can be considered a partial system reset. The open-loop nature of the system to which SILC is applied does not change.

The total topography error is defined as

$$\mathbf{e}_{fb,k} = \sum_{n=1}^{k} \Delta\mathbf{g}_{d,n} - \mathbf{g}_k \tag{12}$$

and is used to determine whether a feedback pass is required. Note that this error is different from the layer-wise SILC error $\mathbf{e}_j$ (6). If the Frobenius norm of the total topography error $\|\mathbf{e}_{fb}\|$ of an ILC layer is larger than the threshold value e_t, a feedback action is introduced between the iterations. This feedback action is given by:

$$\mathbf{u}_{k+1} = \mathbf{f}_{j+1} + \mathbf{C}\mathbf{e}_{fb,k} \tag{13}$$

where $\mathbf{f}_{j+1}$ is the most recent SILC signal as defined in (5) and $\mathbf{C}\mathbf{e}_{fb,k}$ is the feedback signal. The topography update for the feedback pass is given by:

$$\mathbf{g}_j = \mathbf{g}_{k+1} = \mathbf{g}_k + \mathbf{H}(\mathbf{g}_k)\mathbf{u}_{k+1} \tag{14}$$

Note that $\mathbf{g}_{k+1}$ acts as an replacement of $\mathbf{g}_k$. After this feedback action, the SILC resumes according to (5).

4.5 Controller choice

The goal of the feedback controller $\mathbf{C}$ is to reduce the past error as much as possible with a single input, because each input costs one SILC iteration, and the number of iterations within one part is limited by the total height of the part as is shown in Fig. 2. Since the feedback action can be seen as a system reset that occurs outside of the actual SILC loop, the choice of $\mathbf{C}$ does not influence the convergence or stability properties of the SILC loop.

One option is to use the inverse of the estimated spatial impulse response of the system. However, the spatial impulse response on a certain topography is typically difficult to estimate. A second option is to use a simple proportional controller. These controllers typically require multiple passes to reduce the error to zero, but a single pass with a simple controller is expected to reduce the error enough to get below the threshold value. A suitable proportional gain of the controller can be determined experimentally.

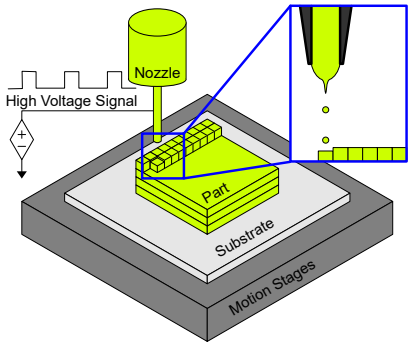

Fig. 4. Schematic representation of e-jet printing.

Table 1. Update law simulation parameters

Norm-optimal weights	$\|\mathbf{L}_f - \mathbf{L}_e\bar{\mathbf{H}}\|$
$q = 1,\ s = 1,\ r = 1$	0.54
$q = 1,\ s = 0.2,\ r = 1$	0.85
$q = 1,\ s = 0.2,\ r = 2$	0.92

5. SIMULATIONS

To determine the feasibility of the proposed multi-layer SILC framework, it is applied to an e-jet printing system in simulation. In this section the simulated e-jet system and the simulation parameters are presented. Then, the results are evaluated based on the traditional ILC criteria of convergence and final topography error. Lastly, alternative performance criteria regarding the total part are presented.

5.1 System setup

An e-jet printer is a microscale additive manufacturing system consisting of a conducting nozzle and substrate, a high-voltage power supply and translational stages as shown in Fig. 4 (Barton et al. (2010)). A pulsed voltage potential between the nozzle and the substrate is used to extract drops from the nozzle. The pulse width of the voltage potential is used to modulate the drop volume (Mishra et al. (2010)).

In the simulation, a layer is printed (4) and measured to determine the error (6) as well as the next iteration input (5). To determine whether a feedback pass is necessary, the norm of the total topography error (12) is compared to the error threshold value.

The linear regression method presented in (Pannier et al. (2019)) is used to generate the topography-dependent nominal model $\bar{\mathbf{H}}$ and simulated physical plant $\mathbf{H}(g_j)$. The spatial impulse response of a droplet deposited on a flat layer of thinly deposited ink is chosen as the nominal behavior on which the learning filters are based. After one part has been printed, the data from the last SILC iteration from the previous part is used to determine the new input. As a result the input converges over multiple parts.

5.2 SILC update law and feedback law design

The reference used for the simulations is a layer with a flat inner part of 256×256 pixels with a height of 0.5 µm and a

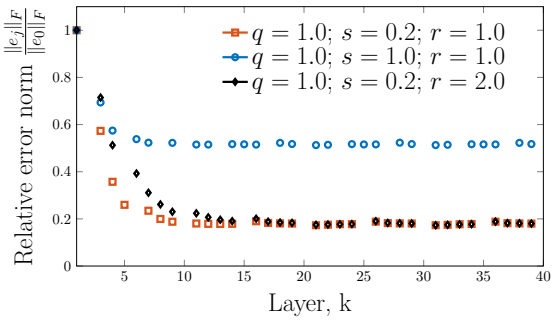

Fig. 5. SILC convergence for a system with feedback passes. The SILC behavior can be influenced by tuning the cost function weighting matrices $\mathbf{Q} = q\mathbf{I}$, $\mathbf{S} = s\mathbf{I}$ and $\mathbf{R} = r\mathbf{I}$.

two-pixel wide border with decreased height as the spread of ink prevents the printing of large height increments. One part consists of ten of these layers, resulting in a total average part height of 4.85 µm. For each simulation four parts are printed, totalling 40 layers.

To simulate the variation of the e-jet system, noise is added to the input signal. The noise is normally distributed with a mean of 0 and a standard deviation of 0.03, approximately $1/8^{\text{th}}$ of the mean value of the nominal input $\bar{\mathbf{f}}$. The reason for choosing normally distributed noise is the assumption that smaller errors in the printing process are more common than larger errors. Since additive manufacturing systems cannot remove material in the previously printed layers, any negative values in the input signal are set to zero.

Different learning filter weights are used to determine their influence on the convergence behavior of the system. All filters are selected to satisfy $\|\mathbf{L}_f - \mathbf{L}_e\bar{\mathbf{H}}\| \leq \gamma < 1$ as shown in Table 1. This guarantees monotonic convergence for the nominal system. However, the values of $\mathbf{H}_j$ are iteration-varying so convergence is not guaranteed. To deal with these variations, learning weights that give robust filters are used.

The controlled system behavior with and without feedback is compared. For the feedback signal, a simple proportional controller with a gain of 2 is used. The threshold value for the Frobenius norm of the error is $e_t = 80$, which is approximately $2/3^{\text{rd}}$ of the initial error. To ensure that each part contains a minimum number of SILC learning passes, a second feedback pass in a row is not permitted. An exception is the the last pass, which is always a feedback pass.

5.3 Evaluation of convergence and final error

All update laws satisfy the monotonic convergence condition for nominal system behavior. Increasing the value of s increases the final error $\mathbf{e}_\infty$ (11), while lowering it increases γ and ultimately leads to an unstable update law due to presence of disturbances. Increasing r reduces the convergence speed, and decreasing it results in instability. The convergence behavior for the different weights in Table 1 is shown in Fig. 5.

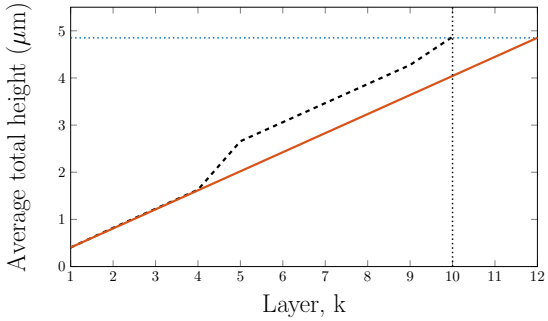

Fig. 6. With feedback (- -), the target height h_{des} (···) of 4.85 µm is reached after the target number of ten layers (···). Without feedback (—), twelve layers are needed to reach this height, exceeding the target number of layers ($q = 1$, $s = 0.2$, $r = 1$).

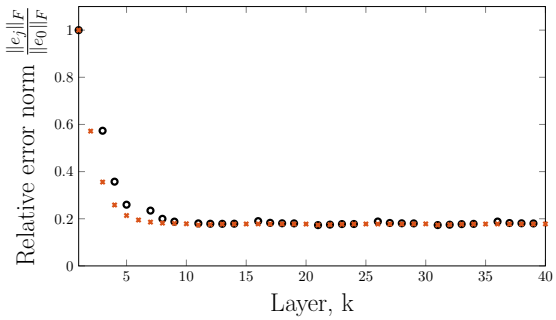

Fig. 7. With feedback (○), more layers are required for the single layer topography error $\mathbf{e}_j$ to converge than without feedback (×) ($q = 1$, $s = 0.2$, $r = 1$).

Two different error metrics are considered. The error for a single layer $\mathbf{e}_j$ is reduced over iterations using SILC and converges to a nonzero final value. As a result, the total topography error $\mathbf{e}_{fb}$ after the target number of ten passes is nonzero, and the final height of the part is lower than the target height. Introducing feedback passes reduces the total topography error, as shown in Fig. 6. Since feedback layers cannot be used for learning, in the approach with feedback the convergence of the single layer error $\mathbf{e}_j$ requires more layers. This is shown in Fig. 7. The converged error value is not influenced by the feedback.

5.4 Alternative performance criteria

The goal of this multi-layer SILC is to print a part, for which the important parameters are the final height of the part and the roughness of the surface. Even if the final error for a layer is nonzero, the final height can still be reached using extra layers as is shown in Fig. 6. The final height of the part can be approximated by the mean value of the final topography. The roughness of the surface is determined by the standard deviation σ of the middle part of the last layer. In Table 2, the values of these criteria, as well as the number of layers required to reach the final height, are given for the different norm-optimal update laws with and without feedback. All values are based on the third printed part because all learning strategies have converged at that point.

Table 2. Update laws compared using AM-specific criteria

Approach	Final height [µm]	σ [µm]	Layers [-]
NO + fb: $q = 1.0$, $s = 1.0$, $r = 1.0$	4.85	0.043	10
NO + fb: $q = 1.0$, $s = 0.2$, $r = 1.0$	4.87	0.034	10
NO + fb: $q = 1.0$, $s = 0.2$, $r = 2.0$	4.87	0.033	10
NO: $q = 1.0$, $s = 1.0$, $r = 1.0$	4.85	0.019	20
NO: $q = 1.0$, $s = 0.2$, $r = 1.0$	4.85	0.015	12
NO: $q = 1.0$, $s = 0.2$, $r = 2.0$	4.85	0.016	12
Target	4.85	0	**10**

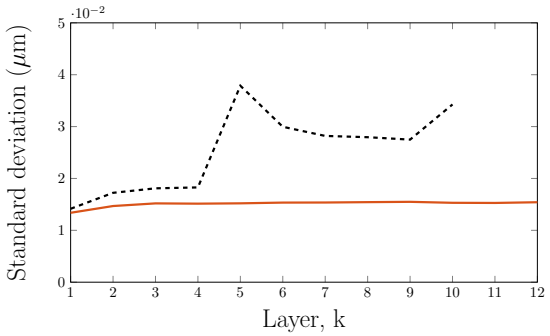

Fig. 8. With feedback (- -) the standard deviation of the topography is increased significantly compared to the case without feedback (—) ($q = 1$, $s = 0.2$, $r = 1$).

When feedback is used, the target height is reached in the target number of layers. Without feedback, the required number of layers depends on the value of the converged error. The influence of the update law on the final height is small.

The standard deviation over layers within one part for cases with and without feedback is shown in Fig. 8. Without feedback, the standard deviation is asymptotic and reaches its final value after approximately four iterations. Feedback passes at $k = 5$ and $k = 10$ of part three cause an increase in the standard deviation. After the feedback pass, the standard deviation decreases. Since update laws with a higher converged error result in more feedback passes, the standard deviation, and therefore the surface roughness of the final part, is higher for these update laws (Table 2).

The simulations show the feasibility of the vertical multi-layer SILC approaches with and without feedback. Feedback avoids an increase in the number of layers; however, feedback increases the standard deviation of the final layer. The reduction in convergence speed and monotonicity caused by feedback is negligible.

6. CONCLUSIONS

This work shows that for multi-layer parts with repeating layers, it is possible to learn within the part by defining each layer as one SILC iteration. Simulations show that the addition of feedback allows the part to reach the target height in the target number of iterations. However, adding feedback also increases the variation in layer topography.

This approach can be used to manufacture multi-layer parts using microscale additive manufacturing. In future work, we aim to define learning in parts that consist of both repeating and unique layers, since many optical, acoustic and electronic applications can be built that way. The implementation of LPV models as those in Pannier et al. (2019) in SILC, for example by using iteration-varying learning filters, offers interesting perspectives as well.

REFERENCES

B. Altin, J. Willems, T. Oomen, and K. Barton. Iterative Learning Control of Iteration-Varying Systems via Robust Update Laws with Experimental Implementation. *Control Engineering Practice*, vol. 62, 36–45, May 2017.

K. Barton, S. Mishra, K.A. Shorter, A. Alleyne, P. Ferreira, and J. Rogers. A desktop electrohydrodynamic jet printing system. *Mechatronics*, vol. 20, 611–616, 2010.

W. Carter, G.C. Popell, J. Samuel, and S. Mishra. A Fundamental Study and Modeling of the Micro-Droplet Formation Process in Near-Field Electrohydrodynamic Jet Printing *J. of Micro- and Nano-Manufacturing*, vol. 2, June 2014.

S. Gunnarsson and M. Norrlöf. On the Design of ILC Algorithms Using Optimization *Automatica*, vol. 37, 2011–2016, 2001.

Y. Guo, J. Peters, T. Oomen, and S. Mishra. Distributed Model Predictive Control for Ink-Jet 3D Printing. *IEEE Int. Conf. on Advanced Intelligent Mechatronics*, July 2017.

D.J. Hoelzle and K.L. Barton. On Spatial Iterative Learning Control via 2-D Convolution: Stability Analysis and Computational Efficiency. *IEEE Trans. Control Syst. Technol.*, vol. 24, no. 4, July 2016.

D. Meng and K.L. Moore. Robust Iterative Learning Control for Nonrepetitive Uncertain Systems. *IEEE Trans. Autom. Control*, vol. 62, no. 2, Feb. 2017.

S. Mishra, K.L. Barton, A.G. Alleyne, P.M. Ferreira, and J.A. Rogers. High-speed and drop-on-demand printing with a pulsed electrohydrodynamic jet. *J. of Micromechanics and Micro-Eng.*, vol. 20, Aug. 2010.

M.S. Onses, E. Sutanto, P.M. Ferreira, A.G. Alleyne, and J.A. Rogers. Mechanisms, Capabilities, and Applications of High-Resolution Elecrohydrodynamic Jet Printing. *Small*, vol. 1, issue 34, June 2015.

C. Pannier, M. Wu, D. Hoelzle, and K. Barton. LPV Models for Jet-Printed Heightmap Control. *Amer. Control Conf.* (Accepted), 2019.

C.P. Pannier, M. Diagne, I.A. Spiegel, D.J. Hoelzle, and K. Barton. A Dynamical Model of Drop Spreading in Electrohydrodynamic Jet Printing. *J. of Manufacturing Science and Engineering*, vol. 139, Nov. 2017.

P. Sitthi-Amorn, J.E. Ramos, Y. Wang, J. Kwan, J. Lan, W. Wang, and W. Matusik. MultiFab: A Machine Vision Assisted Platform for Multi-Material 3D Printing. *ACM Trans. Graphics*, vol. 34, 2015.

Z. Wang, C. Pannier, K. Barton, and D.J. Hoelzle. Application of Robust Monotonically Convergent Spatial Iterative Learning Control to Microscale Additive Manufacturing. *Mechatronics*, vol. 56, 2018a.

Z. Wang, P.M. Sammons, C.P. Pannier, K. Barton, and D.J. Hoelzle. System Identification of a Discrete Repetitive Process Model for Electrohydrodynamic Jet Printing. *Amer. Control Conf.*, 2018b.